Identification of two novel heterodimeric ABC transporters in melanoma: ABCB5β/B6 and ABCB5β/B9

Louise Gerard[1], Laurent Duvivier[1], Marie Fourrez[1], Lindsay Sprimont[1], Michael Gottesman[2], Jean-Pierre Gillet[1]*

[1]Laboratory of Molecular Cancer Biology, URPhyM, NARILIS, University of Namur, Namur, Belgium

[2]Laboratory of Cell Biology, Center for Cancer Research, National Cancer Institute, National Institutes of Health, Bethesda, Maryland, USA

*Correspondence and request for materials should be addressed to Jean-Pierre Gillet, Laboratory of Molecular Cancer Biology, URPhyM, NARILIS, University of Namur, Namur, Belgium. E-mail: jean-pierre.gillet@unamur.be

Abstract

ABCB5 is a member of the ABC transporter superfamily composed of 48 transporters, which have been extensively studied for their role in cancer multidrug resistance and, more recently, in tumorigenesis. ABCB5 has been identified as a marker of skin progenitor cells, melanoma, and limbal stem cells. It has also been associated with multidrug resistance in several cancers. The unique feature of ABCB5 is that it exists as a full transporter (ABCB5FL) and as a half transporter (ABCB5β). Several studies have shown that the ABCB5β homodimer does not confer multidrug resistance, in contrast to ABCB5FL. In this study, using three complementary techniques, nanoluciferase-based bioluminescence resonance energy transfer (NanoBRET), co-immunoprecipitation, and a proximity ligation assay, we identified two novel heterodimers in melanoma: ABCB5β/B6 and ABCB5β/B9. These results represent an important step forward in untangling the functional role of ABCB5β in melanocytes and melanoma.

Introduction

ABCB5 is an ATP-binding cassette (ABC) transporter that belongs to one of the largest and most ancient superfamilies of proteins found in all living organisms. Mammalian ABC proteins are classified into seven families from A to G based on sequence homology[1]. In humans, ABC transporters are mostly exporters, with the exception of ABCA4[2] and ABCD4[3], which function as importers. They exist as full transporters composed of two transmembrane domains (TMDs) and two nucleotide binding domains (NBDs) or as half transporters with one TMD and one NBD, which must either homodimerize or heterodimerize to become functional. However, not all are transporters, ABCE and ABCF members exist as twin NBDs without TMDs and are involved in mRNA translation control[4]. In the ABCC family, ABCC7 is an ATP-gated chloride channel, also known as the cystic fibrosis transmembrane conductance regulator (CFTR)[5], while ABCC8 and ABCC9 serve as regulatory subunits of the ATP-sensitive potassium channel (Kir6.x)[6].

ABCB5 has been highlighted for its role as a marker of skin progenitor cells[7] and melanoma stem cells[8] and, more recently, as a marker of limbal stem cells[9]. It has also been reported to be a mediator of multidrug resistance in melanoma[10], breast cancer[11], colorectal cancer[12,13], hepatocellular carcinoma[14], and several hematological malignancies[15,16]. However, despite these reports, ABCB5 remains poorly characterized. Several transcripts of human ABCB5 have been identified. According to the AceView program, which provides a strictly cDNA-supported view of the human transcriptome and the genes, ABCB5 gene transcription gives rise to at least 11 different transcript variants[17]. Among these, three variants have been documented. In chronological order: ABCB5.b[18] (812 aa, also referred to as ABCB5β), ABCB5.h[19] (131 aa, also referred to as ABCB5α), and ABCB5.a[20] (1257 aa, also referred to as ABCB5FL Full-Length).

ABCB5β was predicted to have a TMD composed of six α-helices flanked by two intracellular NBDs[21]. Conventional half transporters possess only one NBD, either at the N- or the C-terminal region[22]. The ABCB5β N-terminal NBD lacks the Walker A motif, which precludes the binding of ATP. However, ABCB5β might form a dimer to create a functional transporter. Potential dimerization motifs were identified in its N-terminal region[21]. Nevertheless, it has been shown in the yeast model *S. cerevisiae* and also in mammalian cells that an ABCB5β homodimer cannot confer drug resistance[20,23]. These studies focused on a limited number of drugs; therefore, we may not exclude the possibility that this homodimer might be involved in

drug resistance or biological functions that have yet to be unraveled. Yet, it is also worth considering that ABCB5β could dimerize with other half-transporters of the ABCB family to become functional.

Interestingly, ABCB5β belongs to a family that comprises both full and half transporters. These latter include ABCB2/TAP1, ABCB3/TAP2, ABCB6, ABCB7, ABCB8, ABCB9/TAPL, and ABCB10. The first two, ABCB2 and ABCB3, are known to associate in the membrane of the endoplasmic reticulum (ER) to transport peptides from the cytoplasm into the ER lumen, where they are associated with the major histocompatibility complex (MHC) class I molecules for presentation to T-lymphocytes[24]. Furthermore, ABCB7 and ABCB10 have been shown to form a complex with ferrochelastase in the mitochondria, where they are implicated in heme biosynthesis[25].

The three remaining half transporters have been shown to be involved in multidrug resistance in several cancer types, including melanoma[26-28]. Bergam and colleagues demonstrated that ABCB6 is involved in the early steps of melanogenesis[29]. Furthermore, mutations in this gene are responsible for dyschromatosis universalis hereditaria, a rare pigmentary genodermatosis[30]. For ABCB5 and ABCB8, a role in transport of melanin metabolites has been proposed[31]. These transporters could mediate the sequestration of toxic melanin metabolites into lysosomes or melanosomes thereby protecting melanocytes. In melanoma, they could sequester drugs in these organelles[32]. To date, no strong experimental evidence supports these assumptions. Considering that several ABCB half transporters form functional heterodimers, we hypothesized that ABCB5β might heterodimerize with other related members of the ABCB family, possibly, ABCB6, B8 or B9.

In this study, we have identified two novel heterodimeric ABC transporters in melanoma, ABCB5β/B6 and ABCB5β/B9, using three complementary techniques: nanoluciferase-based bioluminescence resonance energy transfer (NanoBRET), co-immunoprecipitation, and proximity ligation assay (PLA). This discovery paves the way for a better understanding of the roles played by these transporters in melanoma.

Results

NanoBRET assay reveals ABCB6 and ABCB9 as interacting partners of ABCB5β

We hypothesized that ABCB5β might heterodimerize with a half transporter of the ABCB family. The review of the literature, already showing ABCB2-ABCB3 and ABCB7-ABCB10 heterodimerization, led us to pinpoint three half transporters, known as ABCB6, ABCB8, and ABCB9 as possible partners for ABCB5β. To study putative interactions between ABCB5β and these proteins, we carried out a NanoBRET assay, described in **Supplementary Fig. 1**. Each of the four proteins was tagged with either a NanoLuc donor or HaloTag acceptor at either the amino (N) or carboxy (C) terminus of the protein, resulting in 16 constructs and eight potential donor/acceptor combinations for each protein pair **(Supplementary Fig. 1B)**. For each combination to be tested, two constructs (one with NanoLuc and one with HaloTag) were transfected in HEK-293T cells, and the fluorescent NanoBRET HaloTag 618 Ligand or DMSO vehicle was added to the cells. Then, the NanoBRET NanoLuc substrate was added, and donor and acceptor signals were measured, which allowed us to calculate a NanoBRET ratio by dividing the acceptor emission value by the donor emission value for each sample in both conditions. To factor in the donor-contributed background, we subtracted the no-ligand control NanoBRET ratio (i.e., DMSO vehicle) from the ligand-containing sample NanoBRET ratio to obtain the corrected NanoBRET ratio **(Supplementary Fig. 1B)**.

We also tested the interaction between additional ABC proteins to control the assay. To this end, we tested the fully characterized ABCB2/B3 heterodimer as a positive control[24]. Further, we tested the putative interactions between ABCB2-ABCD1 and ABCB3-ABCD1 proteins as negative controls, since the ABCB2/B3 heterodimer is expressed in the ER membrane, while ABCD1 is a peroxisomal transporter. We also looked for a putative interaction between ABCB5β-ABCD1 proteins as an additional control.

Each protein pair that was tested yielded a high NanoBRET ratio for one or more donor/acceptor combinations, suggesting heterodimerization (**Supplementary Fig. 1B**). However, variations in transfection efficiency of the donor and acceptor constructs or in constitutive expression of the proteins lead to an environment where the concentrations of all partners are not regulated, rendering any quantitative assumption difficult. Therefore, in this experiment, the NanoBRET ratio was used as qualitative information. Ratios similar to the no-ligand negative control were qualified as noninteracting, and ratios above were qualified as suggesting heterodimerization.

Of note, a drawback of resonance energy transfer assays (e.g., FRET, BRET, and NanoBRET) is that a signal can be detected when proteins are in close proximity but do not interact together[33]. This is often the case for transmembrane proteins, as under overexpression conditions, membrane crowding may lead to protein aggregates that can transfer energy to one another without forming heterodimers. To overcome this limitation, we decided to decrease the amount of donor and acceptor constructs linearly. Nonspecific interaction should lead to decreased NanoBRET ratios, while these should remain stable if the interaction is specific.

For this experiment, we chose the best donor/acceptor combination based on the one that gave the largest NanoBRET ratio (**Supplementary Fig. 1B**). The absence or low signal in other tag combinations for a tested pair indicates that the tags might be too far from one another to transfer energy, not correctly oriented, or they might impair the protein folding, localization, or dimerization[34]. Therefore, the largest NanoBRET ratio represents the pair combination for which both tags are in the best conformation to transfer energy to one another. The selected pairs are highlighted in **Supplementary Fig. 1B**.

HEK-293T cells were transfected with decreasing amounts of NanoLuc (donor) and HaloTag (acceptor) constructs from 1 µg to 0.125 µg for each construct (**Fig. 1**). The NanoBRET ratio decreased along with the DNA amount for ABCB2-ABCD1, ABCB3-ABCD1, and ABCB5β-ABCD1 pairs that were tested as negative controls (**Fig. 1A**), while it remained similar regardless of the amount of DNA transfected for ABCB2-ABCB3 used as a positive control (**Fig. 1B**). Interestingly, NanoBRET ratios remained similar in all conditions for ABCB5β/B6 and ABCB5β/B9, suggesting that these proteins might form true heterodimers. The NanoBRET ratio obtained for the last protein pair, ABCB5β-ABCB8, decreased along with the amount of DNA transfected, similar to the data generated from protein pairs assessed as negative controls.

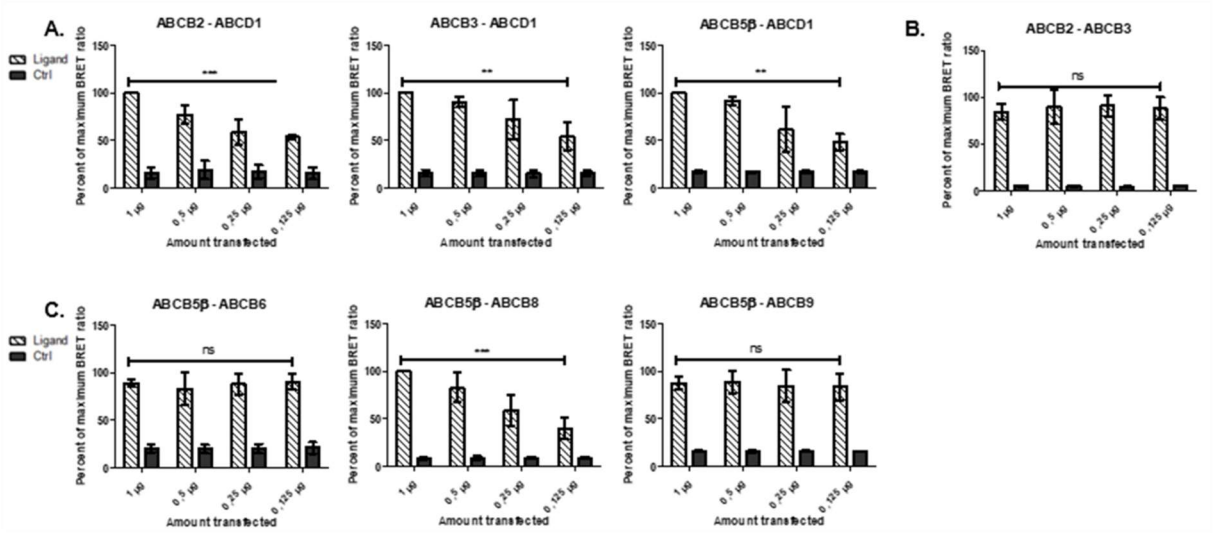

Fig. 1: NanoBRET dilution assay reveals two putative heterodimers, ABCB5β/B6 and ABCB5β/B9. HEK-293T cells were transfected with decreasing amounts of NanoLuc and HaloTag constructs. Transfection started at 1 µg and went down to 0.125 µg per construct. "Ctrl" stands for the technical negative control to which DMSO is added instead of ligand. Proteins pairs serving as negative controls (ABCB2-ABCD1, ABCB3-ABCD1, ABCD1-ABCB5β) (**A**) and a positive control pair (ABCB2-ABCB3) (**B**) were tested along with ABCB5β-ABCB6, ABCB5β-ABCB8, and ABCB5β-ABCB9 (**C**). Data are presented as mean ± SD. Simple linear regression was used to test if the amount transfected significantly influenced the NanoBRET ratio (n = 3). P-values are represented on graphs as *** $p<0.001$, ** $p<0.01$, and $p>0.05$. For ABCB2-ABCD1 (R^2 = 0.8719, $F(1,10)$ = 68.07), ABCB3-ABCD1 (R^2 = 0.6144, $F(1,10)$ = 15.94), ABCB5β-ABCD1 (R^2 = 0.6661, $F(1,10)$ = 19.95), and ABCB5β-ABCB8 (R^2 = 0.7526, $F(1,10)$ = 30.41), the relation between both parameters was statistically significant. For ABCB2-ABCB3 (R^2 = 0.0269, $F(1,10)$ = 0.2767), ABCB5β-ABCB6 (R^2 = 0.0011, $F(1,10)$ = 0.0113), and ABCB5β-ABCB9 (R^2 = 0.0204, $F(1,10)$ = 0.2080), changes in the amount of transfected DNA did not influence the NanoBRET ratio.

Donor saturation assay confirms the specificity of the interaction between ABCB5β/B6 and ABCB5β/B9 protein pairs

To confirm the specific interaction of ABCB5β-ABCB6 and ABCB5β-ABCB9 protein pairs and the false positive signals of ABCB5β-ABCB8, ABCB2-ABCD1, ABCB3-ABCD1, and ABCB5β-ABCD1 protein pairs, a saturation assay was performed in HEK-293T cells (**Fig. 2**). In this experiment, the amount of donor construct was held constant, while the amount of acceptor construct was increased. For this assay, the smallest concentrations of donor and acceptor showing heterodimerization were used. If the interaction between both proteins is specific, the NanoBRET signal will increase in a hyperbolic manner and reach a plateau where

all the donors are saturated with the acceptors, and luminescence can no longer increase. On the other hand, for a nonspecific interaction, the signal will continue to increase linearly with an increasing amount of acceptor (**Fig. 2A**). At these concentrations, signal from nonspecific interaction will not reach a plateau due to the lack of affinity between proteins.

We carried out this donor saturation assay on the ABCB2-ABCB3 protein pair used as a positive control and compared the data with the three protein pairs chosen as negative controls. As shown in **Fig. 2B**, the NanoBRET signal was saturable for the ABCB2-ABCB3 protein pair, while a linear increase was observed for ABCB2-ABCD1, ABCB3-ABCD1, and ABCB5β-ABCD1 protein pairs. This supports the specificity of the interaction for the ABCB2-ABCB3 protein pair. Then, we assessed the specificity of the interaction for the three protein pairs of interest, and the analysis of the data revealed a hyperbolic increase in the NanoBRET signal that eventually reached a plateau phase for both ABCB5β-ABCB6 and ABCB5β-ABCB9 protein pairs, similar to what was observed for the positive control. On the contrary, the donor saturation assay further supported a nonspecific interaction between ABCB5β and ABCB8 proteins (**Fig. 2C**).

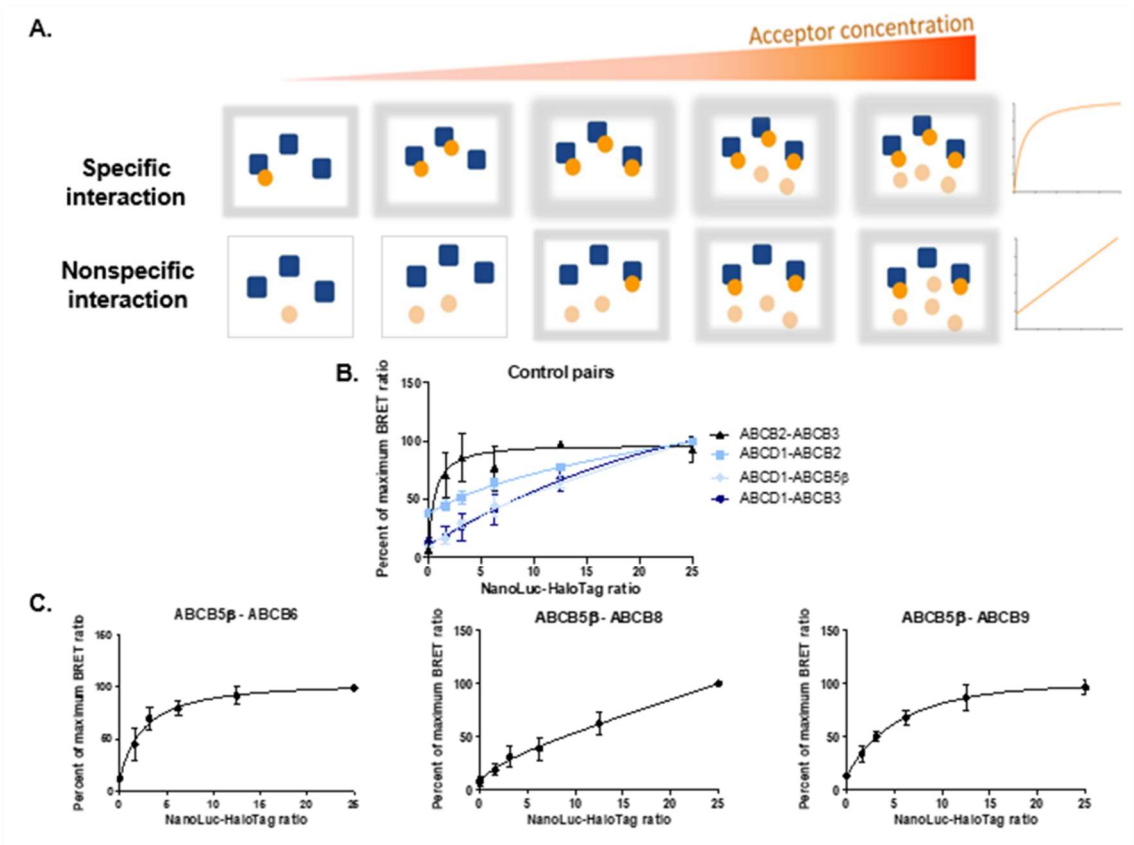

Fig. 2: Saturation assay confirms ABCB5β-ABCB6 and ABCB5β-ABCB9 specific interactions. **(A)** Concentration of donor is held constant while concentration of acceptor is increased. If the interaction is specific, the signal will reach a plateau where all the donors are saturated with acceptor, and luminescence will no longer increase. On the other hand, for a nonspecific interaction, the signal will continue to increase linearly. For each square, the schematic gray halo represents the intensity of the NanoBRET signal observed from low to high. In graphs (**B-C**), the percent of the maximum NanoBRET ratio is plotted against the NanoLuc−HaloTag ratio. (**B)** Donor saturation assay for positive, ABCB2-ABCB3, and negative, ABCB2-ABCD1, ABCB3-ABCD1, ABCB5β-ABCD1, controls. (**C)** Donor saturation assay for ABCB5β-ABCB6, ABCB5β-ABCB8, and ABCB5β-ABCB9.

Co-immunoprecipitation and proximity ligation assay confirm interactions between ABCB5β-ABCB6 and ABCB5β-ABCB9 protein pairs

Co-immunoprecipitation (Co-IP) is considered one of the standard methods of identifying or confirming the occurrence of protein-protein interaction events. So, as a first step, we used HEK-293T cells that constitutively express ABCB6 and ABCB9. Since the expression of ABCB5β had not been demonstrated in this cell line, we transfected them with mCherry-tagged ABCB5β (**Supplementary Fig. 2**). Proteins of interest were immunoprecipitated using either an anti-mCherry, ABCB5, ABCB6, or ABCB9 antibody, and their interacting partners were analyzed by western blotting after SDS-PAGE using corresponding antibodies to show protein−protein interaction (**Supplementary Fig. 2**). An isotype control was performed to determine the specificity of the signal obtained in the western blots.

Membrane protein overexpression and the presence of a tag may lead to various issues, including membrane crowding, protein mislocalization, protein misfolding, or protein loss of function. Therefore, we decided to work with Mel JuSo and UACC-257, two melanoma cell lines that constitutively express the target proteins (**Fig. 3**). Immunoprecipitation with either an anti-ABCB5, ABCB6, or ABCB9 antibody brings out the interacting partners, which can be identified by western blotting following an SDS-PAGE using the corresponding antibody. The data presented in **Fig. 3** further supports the occurrence of interaction between ABCB5β-ABCB6 and ABCB5β-ABCB9 protein pairs (**Fig. 3**).

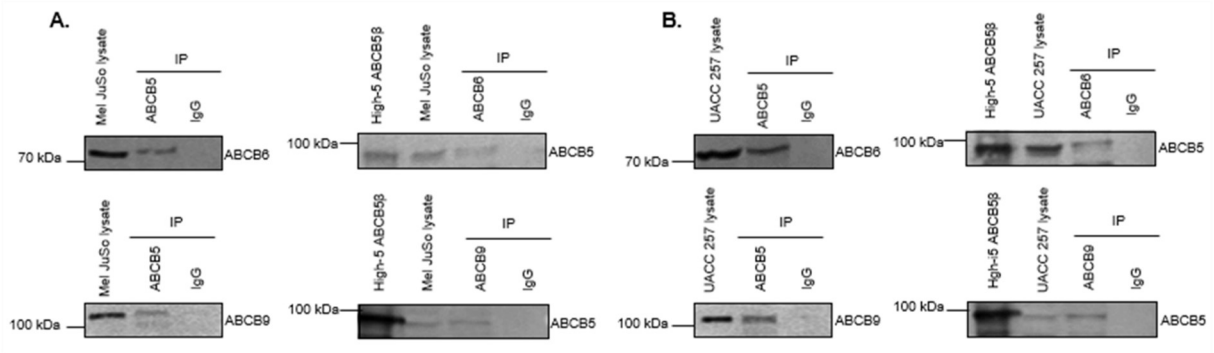

Fig. 3: Co-immunoprecipitation of ABCB5β-ABCB6 and ABCB5β-ABCB9 indicates that these heterodimers are found in Mel JuSo and UACC-257 cells. Mel JuSo (**A**) or UACC-257 (**B**) proteins were immunoprecipitated (IP) with an anti-ABCB5, anti-ABCB6, or anti-ABCB9 antibody. The precipitated proteins were revealed by western blotting after SDS-PAGE using the corresponding antibody indicated on the right side of each blot. Fifteen µg of proteins from the starting cell lysate were loaded in the first lane and the total IP eluate was loaded on the gel. ABCB5β was expressed in High Five insect cells, and crude membrane proteins were prepared and loaded on the gel (High5 ABCB5β) as a complementary molecular weight marker when using anti-ABCB5. An isotype control was performed to determine the specificity of the signal obtained in western blot.

In situ validation of the interactions for these two protein pairs was obtained using a proximity ligation assay (PLA) in Mel JuSo and UACC 257. The PLA principle is illustrated in **Supplementary Fig. 3**. For ABCB5β-ABCB6 and ABCB5β-ABCB9, strong red PLA signals could be detected, consistent with interactions between the studied protein pairs (**Fig. 4A**). To further assess the specificity of the PLA signal, multiple controls were performed. Biological controls were conducted in which Mel JuSo and UACC-257 cell lines were produced that stably expressed either a nontargeting short hairpin RNA (shRNA) or an ABCB6-specific (or ABCB9-specific) shRNA. **Fig. 4B and C** show the resulting decrease of expression at the mRNA and protein levels). In both cell lines, stable knockdown of ABCB6 or ABCB9 resulted in a statistically significant decrease in PLA signal ($p<0.0001$) compared with nontargeting shRNA counterparts (**Fig. 4D**). Technical controls were also conducted without adding one of the two antibodies directed against the proteins of interest, and without adding both antibodies (**Fig. 4D**).

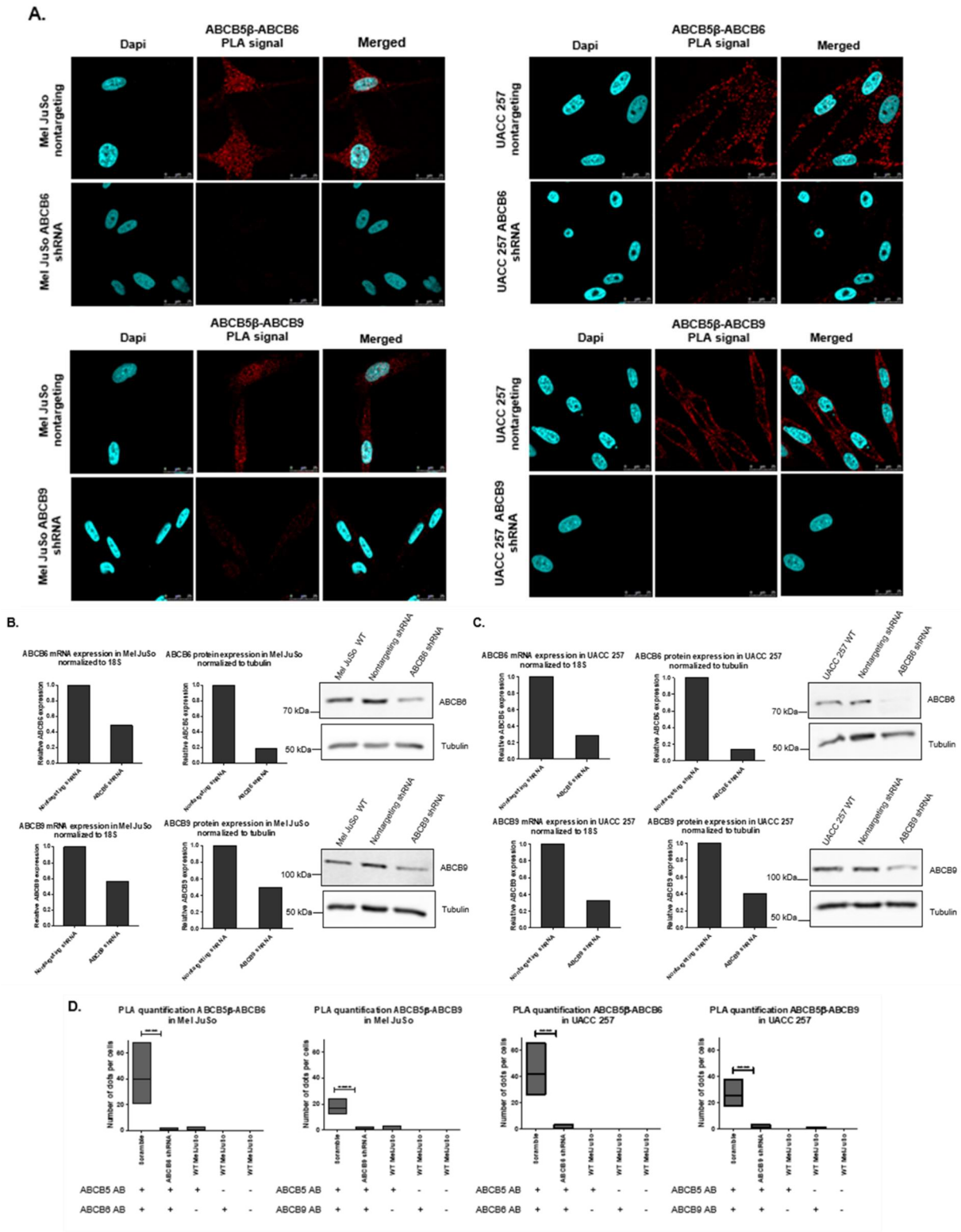
A.
ABCB5β-ABCB6 PLA signal
Dapi
Merged
Mel JuSo nontargeting
Mel JuSo ABCB6 shRNA
UACC 257 nontargeting
UACC 257 ABCB6 shRNA
ABCB5β-ABCB9 PLA signal
Mel JuSo ABCB9 shRNA
UACC 257 ABCB9 shRNA
B.
ABCB6 mRNA expression in Mel JuSo normalized to 18S
ABCB6 protein expression in Mel JuSo normalized to tubulin
ABCB9 mRNA expression in Mel JuSo normalized to 18S
ABCB9 protein expression in Mel JuSo normalized to tubulin
Mel JuSo WT
Nontargeting shRNA
ABCB6 shRNA
ABCB9 shRNA
70 kDa
50 kDa
100 kDa
ABCB6
ABCB9
Tubulin
C.
ABCB6 mRNA expression in UACC 257 normalized to 18S
ABCB6 protein expression in UACC 257 normalized to tubulin
ABCB9 mRNA expression in UACC 257 normalized to 18S
ABCB9 protein expression in UACC 257 normalized to tubulin
UACC 257 WT
D.
PLA quantification ABCB5β-ABCB6 in Mel JuSo
PLA quantification ABCB5β-ABCB9 in Mel JuSo
PLA quantification ABCB5β-ABCB6 in UACC 257
PLA quantification ABCB5β-ABCB9 in UACC 257
Number of dots per cells
Scramble
ABCB6 shRNA
ABCB9 shRNA
WT MelJuSo
WT UACC
ABCB5 AB
ABCB6 AB
ABCB9 AB

Figure 4: Proximity ligation assay to confirm interactions between ABCB5β-ABCB6 and ABCB5β-ABCB9 protein pairs in Mel JuSo and UACC 257. (A) Confocal images of PLA in Mel JuSo and UACC 257 that stably expressed either a nontargeting short hairpin RNA (shRNA) or an ABCB6-specific (or ABCB9-specific) shRNA. The PLA signal is detected in red. Nuclei are stained in blue using DAPI. After shRNA knockdown, efficiency was determined using RT-qPCR and western blots in Mel JuSo (**B**) and UACC 257 (**C**). 18S and tubulin were used as references for RT-qPCR and the western blots, respectively (n=2). Western blot quantification to assess protein expression was performed using ImageJ. (**D)** Quantification of the average number of dots per cell was determined using ImageJ (n = 3). Scramble and shRNA quantifications are presented along with technical negative controls, including PLA conducted without one antibody (AB) out of the two used or none. Data are presented as mean ± *SD*. In Mel JuSo: ABCB6 scramble (39.89 ± 14.21), ABCB6 shRNA (0.28 ± 0.60), ABCB5 AB control (0.55 ± 0.91), ABCB6 AB control (0 ± 0), ABCB9 scramble (16.89 ± 4.27), ABCB9 shRNA (0.84 ± 1.04), ABCB9 AB control (0 ± 0.01), and no antibody control (0.01 ± 0.05). In UACC 257: ABCB6 scramble (42.16 ± 10.62), ABCB6 shRNA (0.97 ± 1.00), ABCB5 AB control (0.01 ± 0.02), ABCB6 AB control (0.03 ± 0.07), ABCB9 scramble (25.39 ± 6.74), ABCB9 shRNA (1.04 ± 1.16), ABCB9 AB control (0.79 ± 0.58), and no antibody control (0 ± 0). Student's *t*-test was performed between the scramble and shRNA conditions. Statistical significances are presented on graph as ****p<0.0001. ABCB5β/B6 in Mel JuSo (t = 9.648, df = 22), ABCB5β/B9 in Mel JuSo (t = 12,66, df = 22), ABCB5β/B6 in UACC 257 (t = 13,38, df = 22), ABCB5β/B9 in UACC257 (t = 12,34, df = 22).

Discussion

To explore the possible role of the ABCB5β variant, we conducted heterodimerization studies with potential target half transporters of the ABCB family in melanoma. This ABC family comprises three full-length transporters (i.e., ABCB1, B4, and B11) and seven half transporters. Uniquely among all ABCB family transporters, ABCB5 is found as both a full transporter and a half transporter (ABCB5β), in which the expression of each is driven by independent promoters. The current knowledge on these transporters led us to focus on three candidate heterodimers: ABCB5β-ABCB6, ABCB5β-ABCB8, and ABCB5β-ABCB9. Putative interactions between these three pairs of proteins were studied using the NanoBRET assay, and confirmed using co-immunoprecipitation and proximity ligation assay. Taken together, these assays revealed two novel heterodimeric ABC transporters in melanoma.

FRET microscopy in living cells has been applied to unravel the interactions of peroxisomal ABC transporters ABCD1 and ABCD3[35]. In this study, we carried out a NanoBRET assay, which does not require extrinsic excitation and provides substantially increased detection sensitivity and dynamic range compared to current BRET technologies[34]. We demonstrated the

importance of transfecting a low amount of donor and acceptor constructs to avoid membrane crowding, as well as protein aggregates that may lead to false positive BRET signals, as observed for ABCB8-ABCB5β, ABCB2-ABCD1, ABCB3-ABCD1, and ABCB5β-ABCD1 in Supplementary Figure 1B. This so-called bystander signal is the result of two proteins being close enough to transfer energy, but that do not interact together[33]. The donor saturation assay confirmed the specificity of the interaction between ABCB5β-B6 and ABCB5β-B9 protein pairs and demonstrated the nonspecificity of the interactions of the other pairs of proteins. Co-immunoprecipitation was chosen to confirm the occurrence of protein-protein interaction events in the particularly easy-to-transfect HEK-293-T. Since ABCB5β expression had not been shown in these cells, we used mCherry-tagged ABCB5β. This experiment allowed us to confirm the data obtained from the NanoBRET assay using the same cell line. However, to avoid any alteration in protein localization and membrane crowding due to protein tags and protein overexpression, we wanted to assess protein–protein interaction in a relevant model that expresses the three transporters of interest. Since ABCB5β is predominantly expressed in melanoma, we used two melanoma cell lines, Mel JuSo and UACC-257, which also constitutively express ABCB6 and ABCB9. Nevertheless, we wanted to validate the data *in situ* in live melanoma cell lines. Therefore, we carried out a proximity ligation assay in melanoma cell lines that stably express either a nontargeting short hairpin RNA (shRNA) or an ABCB6-specific (or ABCB9-specific) shRNA. Altogether, this set of experiments demonstrates the existence of the two heterodimeric ABC transporters in Mel JuSo and UACC257 melanoma cell lines.

The localization of these two heterodimers must be determined and these studies are currently underway. ABCB6 has a conflicting localization in the literature. This transporter was shown to uniquely localize in the outer membrane of the mitochondria[36], and later, it was reported to localize to both the outer mitochondrial membrane and the plasma membrane[37]. In a more recent study, ABCB6 was reported to have an endolysosomal localization[38]. ABCB9 was shown to go through Golgi, then endosomes, to reach lysosomes[39]. ABCB5β localization remains elusive, but based on its interacting partners, we can hypothesize a localization in lysosome-related organelles.

In conclusion, this study presents the first evidence for two novel ABC transporters formed by the heterodimerization of ABCB5β with ABCB6 or ABCB9 in Mel JuSo and UACC-257 melanoma cell lines. This discovery is a step toward a better understanding of the role of ABCB5β in melanocytes and melanoma.

Methods

Cell culture and transfection

The HEK-293T cell line, a derivative of human embryonic kidney 293 cells, transformed with the SV40 T-antigen, and the Mel JuSo and UACC-257 melanoma cell lines were cultured in DMEM (Lonza, Basel, Switzerland) supplemented with 10% FBS (GE Healthcare Life Sciences, Issaquah, WA, USA) and 1% penicillin/streptomycin (Gibco, Carlsbad, CA, USA) at 37 °C and 5% CO_2 in a humidified atmosphere.

For transient transfection, cells were seeded to reach 70% confluence in a six-well plate. Four hours later, transfection with jetPRIME (Polyplus transfection, Illkirch, France) was carried out following the manufacturer's instructions.

shRNAs constructs for stable knockdown of human ABCB6 (sc-94721-SH) and ABCB9 (sc-60115-SH) were obtained from Santa Cruz Biotechnology (Dallas, TX, USA). A nonsilencing shRNA was used as a control (sc-108060). Reverse transfection was performed in antibiotic-free medium with jetPRIME following the manufacturer's instructions (Polyplus transfection, Illkirch, France). Seventy-two hours after transfection, selection of the transfected cells was carried out by the addition of 2 µg/ml of puromycin. After 10 days of selection, ABCB6 and ABCB9 mRNA and protein expression were assessed using RT-qPCR and western blot.

DNA constructs

ABCB2, ABCB3, ABCB5β, ABCB6, ABCB8, ABCB9, and ABCD1 cDNAs were inserted into the pCDNA3.1 expression vector and subcloned into the NanoLuc pNLF1-N[CMV/Hygro], the NanoLuc pNLF1-C[CMV/Hygro], the HaloTag pHTC HaloTag CMV-neo, and the HaloTag pHTN HaloTag CMV-neo vector purchased from Promega (Madison, WI, USA). Restriction enzymes Not1-EcoR1, Nhe1-EcoR1, Not1-EcoR1, and Nhe1-EcoR1 were used, respectively.

The mCherry-tagged ABCB5 mammalian expression construct (ID: 8488-X02-787) driven by a CMV promoter was provided by Ledios Biomedical Research (formerly SAIC-Frederick, NCI, MD, USA).

RT-qPCR

Total RNA was isolated from Mel JuSo and UACC-257 using a NucleoSpin RNA Plus kit following the manufacturer's instructions (Takarabio, Kusatsu, Japan). Reverse transcription was performed using a High-Capacity cDNA Reverse Transcription kit and 200 ng of total

RNA (Thermo Fisher Scientific, Waltham, MA, USA) according to the manufacturer's instructions. Quantitative PCR was performed using TaqMan master mix (Thermo Fisher Scientific, Waltham, MA, USA) and 18s expression was used to normalize data. The following probes from Thermo Fisher Scientific were used: 18S (Hs03003631_g1), ABCB6 (Hs00180568_m1), and ABCB9 (Hs00608640_m1).

NanoBRET

Twenty-four hours after transient transfection of NanoLuc and HaloTag constructs, the cells were washed with PBS and trypsinized. Cells were counted and diluted in OptiMEM supplemented with 4% FBS to reach a density of 2×10^5 cells/ml. One µl of 0.1 mM HaloTag NanoBRET ligand 618 (Promega, Madison, WI, USA) per ml of cells or DMSO in the control conditions was added. One hundred µl of cells with ligand or DMSO were plated in a 96-well plate (Corning 3917, Thermo Fisher Scientific, Waltham, MA, USA) and were cultured overnight at 37 ˚C, 5% CO_2. Twenty-five µl of 100x dilution of NanoBRET NanoGlo substrate (Promega, Madison, MA, USA) was added per well. Plates were shaken for 30 seconds at 400 rpm and then kept in the dark for 30 seconds. Finally, donor emission (447 nm) and acceptor emission (610 nm) were measured at room temperature using a dual filter (SpectraMax i3x, Molecular Devices, San Jose, CA, USA). For all experiments, biological triplicates were performed. All biological triplicates were composed of technical triplicates.

Relative light units (RLU) obtained for donor and acceptor emission were processed as follows to obtain milli Bioluminescence Units (mBU):

$$\frac{emission\ 610\ \text{nm}}{emission\ 447\ \text{nm}} = BU \times 1000 = mBU$$

For saturation experiments, percentages of maximum NanoBRET ratio were plotted against the acceptor to donor ratio, and data were fitted using the "one site–total and nonspecific binding" fit.

Co-immunoprecipitation

Five mg of proteins in lysis buffer (120 mM NaCl, 50 mM Tris, NP40 0.5%, 5 mM EDTA, 1x protease inhibitor) were incubated on a rotating wheel at 4 °C for 4 hours with 1 µg of antibody: ABCB5 (600-401-A775, Rockland Immunochemicals, Pottstown, PA, USA), ABCB6 (G-10, Santa Cruz Biotechnology, Dallas, TX, USA), ABCB9 (A-8, Santa Cruz Biotechnology, Dallas, TX, USA), IgG Mouse (sc-2025, Santa Cruz Biotechnology, Dallas, TX, USA), and IgG Rabbit (sc-3888, Santa Cruz Biotechnology, Dallas, TX, USA). In the meantime, 25 µl of

magnetic beads, Dynabeads-Protein A (Invitrogen, Waltham, MA, USA) and Dynabeads-Protein G (Invitrogen, Waltham, MA, USA), were added to an Eppendorf and washed twice with 250 µl of lysis buffer using a magnetic rack. Thereafter, protein lysates with antibody were added to the beads and incubated overnight at 4 °C on a rotating wheel. The following day, the beads were washed three times with 250 µl of cold PBS 0.05% Tween 20. Fifty µl of elution buffer (DTT, Tris, Glycerol, SDS) was added, and samples were heated at 40 °C for 10 minutes. Samples were analyzed using western blot.

SDS-PAGE and Western blotting

Samples were loaded on an 8% SDS acrylamide gel, migrated at 110 V, and transferred to a PVDF membrane at 110 V for 1h30. The membrane was blocked for 1 hour in 5% milk diluted in PBS 0.05% Tween 20 and incubated overnight with the following primary antibodies: anti-ABCB5 (600-401-A775, Rockland Immunochemicals, Pottstown, PA, USA), anti-ABCB6 (sc-365930, Santa Cruz Biotechnology, Dallas, TX, USA), anti-ABCB9 (sc-39412, Santa Cruz Biotechnology, Dallas, TX, USA), and anti-mCherry (ab167453, Abcam, Cambridge, UK). Then, membranes were either incubated for 1 hour with Scan Later anti-mouse or anti-rabbit secondary antibodies (Molecular Devices, San Jose, CA, USA), followed by washing with PBS 0.05% Tween 20 and revelation with the SpectraMax i3x (Molecular Devices, San Jose, CA, USA). Alternatively, membranes were incubated for 1 hour with horseradish peroxidase-conjugated goat anti-mouse or anti-rabbit antibodies (Agilent Technologies, Santa Clara, CA, USA), followed by washing with PBS 0.05% Tween and revelation with enhanced chemiluminescence (PerkinElmer, Waltham, MA, USA).

***In situ* proximity ligation assay**

Cells grown on a coverslip were fixed in 4% paraformaldehyde (PFA) for 20 minutes and permeabilized with PBS + Triton X-100 0.2% for 10 minutes. Then, proximity ligation assay (PLA) was performed following Duolink kit (Sigma-Aldrich, Saint Louis, MO, USA). Briefly, the coverslips were incubated with blocking solution for 1 hour at 37 °C in a humidity chamber. Then, they were incubated for 1 hour at room temperature with primary antibody pairs raised against different species (mouse and rabbit) and diluted 1/200: ABCB5β (LS-C169144, LSBio, Seattle, WA, USA), ABCB6 (600-401-945, Rockland Immunochemicals, Pottstown, PA, USA), ABCB8 (ab83194, Abcam, Cambridge, UK), and ABCB9 (PA5-99017, Invitrogen, Waltham, MA, USA). Cells were incubated with PLA probes mouse PLUS and rabbit MINUS for 1 hour at 37 °C. Next, ligation was performed for 30 minutes at 37 °C, followed by

amplification for 100 minutes at 37 °C. Finally, the coverslips were mounted on mounting medium with DAPI (Sigma-Aldrich, Saint Louis, MO, USA). The edges were sealed with clear nail polish. Images were obtained using a Leica TCS SP5 confocal microscope (Leica Microsystems, Wetzlar, Germany). DAPI, argon, and 561 red filters were used. The number of red dots per cell was counted using ImageJ software as described in Gomes et al[40]. Each condition was obtained in biological triplicates.

Statistical analysis

Data were analyzed using GraphPad Prism version 5.04 for Windows with linear regression or unpaired Student's *t*-test. Statistical analysis is indicated in the figures' legends. Statistical significance was defined as $p<0.05$.

Acknowledgments

We thank Simon Lefèvre for initial work on co-immunoprecipitations, and Andy Chevigné of the Department of Infection and Immunity, Luxembourg Institute of Health, for the useful discussion regarding NanoBRET experiments. We are grateful to Vincent Van Hée and Marylène Focant of Promega for their support in the optimization and troubleshooting of the NanoBRET assay. We thank Marielle Boonen (Intracellular Trafficking Biology, NARILIS, UNamur) for her critical reading of the manuscript.

Author contributions

L.G. designed and performed the majority of the experiments and analyzed the data. L.D. prepared the NanoBRET constructs. L.D. and L.S. contributed to the NanoBRET assay optimizations. M.F. performed co-IPs using the mCherry-tagged ABCB5β construct. L.G. and J.P.G. wrote and edited the manuscript. M.G. provided overall direction and helped edit the manuscript. J.P.G. supervised the project and contributed to the design of the experiments and the analysis of the data.

Competing interests

The authors declare no competing interests.

Supplementary information

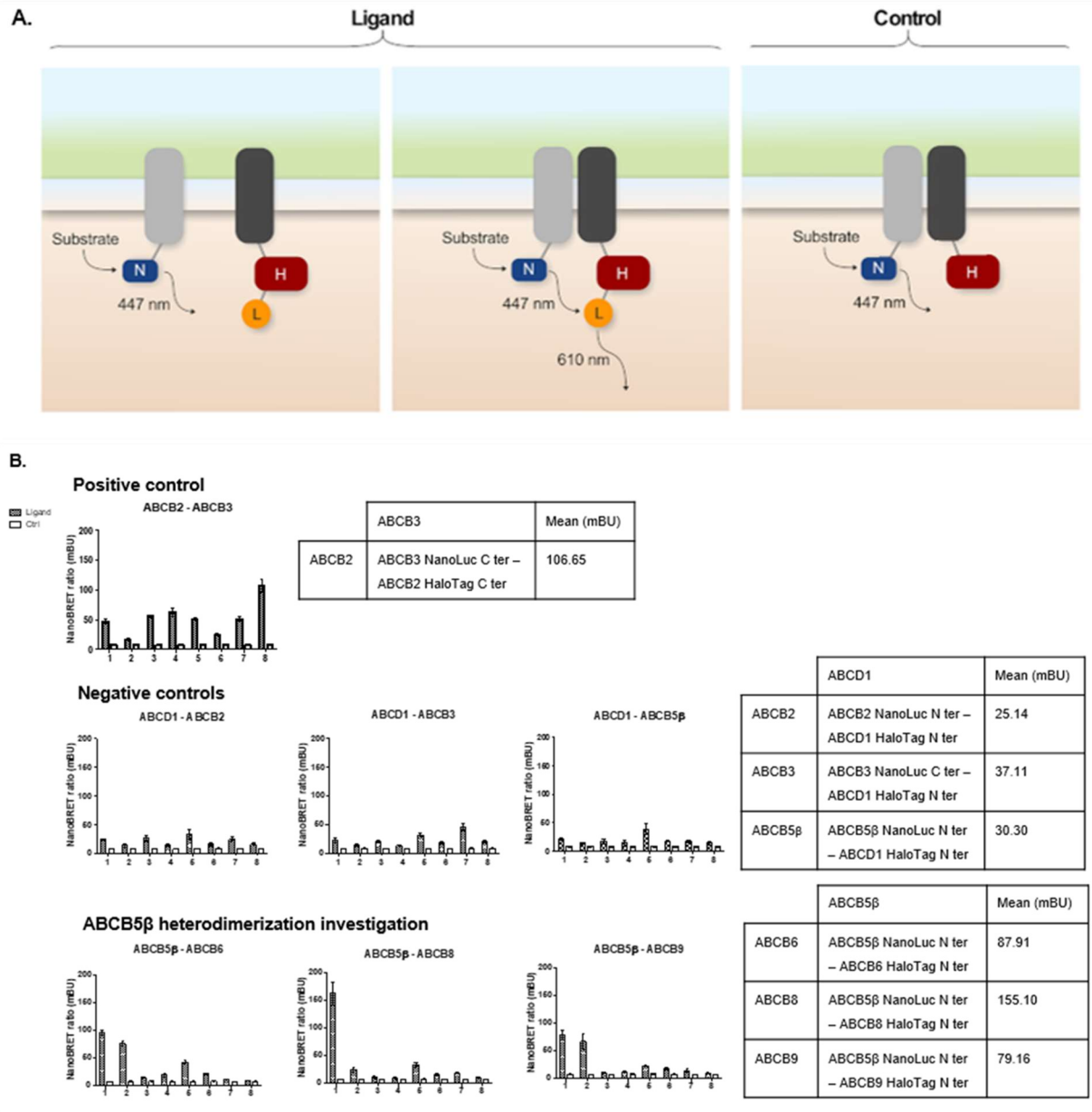

	ABCB3	Mean (mBU)
ABCB2	ABCB3 NanoLuc C ter – ABCB2 HaloTag C ter	106.65

	ABCD1	Mean (mBU)
ABCB2	ABCB2 NanoLuc N ter – ABCD1 HaloTag N ter	25.14
ABCB3	ABCB3 NanoLuc C ter – ABCD1 HaloTag N ter	37.11
ABCB5β	ABCB5β NanoLuc N ter – ABCD1 HaloTag N ter	30.30

	ABCB5β	Mean (mBU)
ABCB6	ABCB5β NanoLuc N ter – ABCB6 HaloTag N ter	87.91
ABCB8	ABCB5β NanoLuc N ter – ABCB8 HaloTag N ter	155.10
ABCB9	ABCB5β NanoLuc N ter – ABCB9 HaloTag N ter	79.16

Supplementary Fig. 1: Schematic representation of the NanoBRET technique and preliminary NanoBRET ratio.

A NanoBRET consists of an engineered luciferase, NanoLuc (N), fused to our transporter of interest. The HaloTag protein (H) is fused to the potential interacting partner. Following substrate addition, NanoLuc emits at 447 nm. If the HaloTag ligand (L), covalently bound to the HaloTag protein, is in close proximity (less than 10 nm), it will be excited by NanoLuc emission, and it will emit at 610 nm. The ratio between the 447 nm and 610 nm signals allows distinction between interacting (i.e., high ratio) and noninteracting proteins (i.e., low ratio, close to the technical negative control). The technical negative control consisted of the same experiment without the ligand. **B** NanoBRET ratio of the positive

control, negative controls, and investigation of putative ABCB5β heterodimerization. ABC transporters were cloned in NanoLuc (N) or HaloTag (H) vector in either N or C terminus, giving eight possible combinations per transporter's pairs. Data are represented as mean ± SD. The order of the combination on each graph is as follows, with ABC 1 being the first ABC transporter mentioned in the graph title and ABC 2 the second: 1) ABC 1 NanoLuc N terminus – ABC 2 HaloTag N terminus, 2) ABC 1 NanoLuc N terminus – ABC 2 HaloTag C terminus, 3) ABC 1 NanoLuc C terminus – ABC 2 HaloTag N terminus, 4) ABC 1 NanoLuc C terminus – ABC 2 HaloTag C terminus, 5) ABC 2 NanoLuc N terminus – ABC 1 HaloTag N terminus, 6) ABC 2 NanoLuc N terminus – ABC 2 HaloTag C terminus, 7) ABC 2 NanoLuc C terminus – ABC 1 HaloTag N terminus, 8) ABC 2 NanoLuc C terminus – ABC 1 HaloTag C. terminus. One µg of NanoLuc and HaloTag constructs was transfected in HEK-293T. Preferred tag orientations selected for further testing in dilution and saturation assays are highlighted in the different tables, along with their mean NanoBRET ratios.

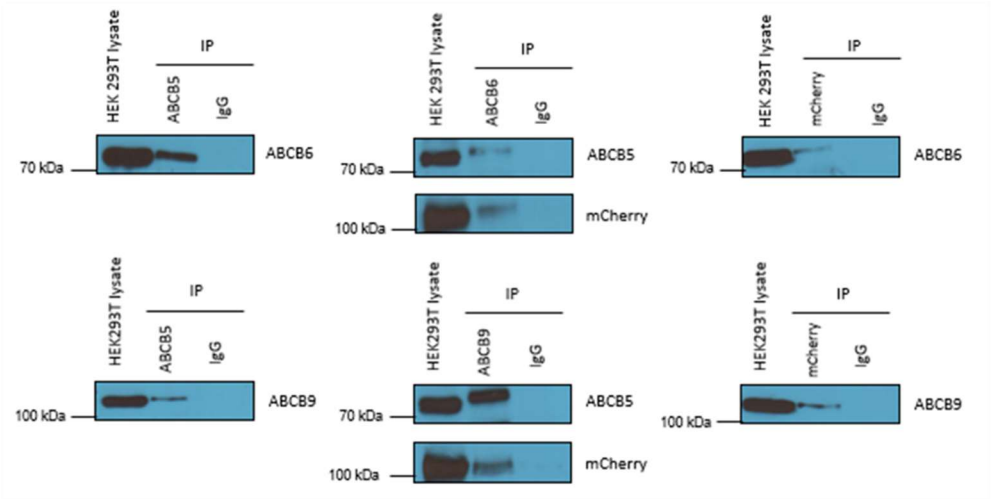

Supplementary Fig. 2: Co-immunoprecipitation of ABCB5β-ABCB6 and ABCB5β-ABCB9 using HEK-293T transfected with the mCherry-tagged ABCB5 construct.

Cell lysates were immunoprecipitated (IP) using an anti-ABCB5, anti-ABCB6, anti-ABCB9, or anti-mCherry antibody. The precipitated proteins were visualized by SDS-PAGE using the corresponding antibody indicated on the right side of each blot. Fifty µg of proteins and the total volume obtained after IP were loaded on the gel for the lysate or IP conditions, respectively. An isotype control was performed to determine the specificity of the signal obtained in the western blots.

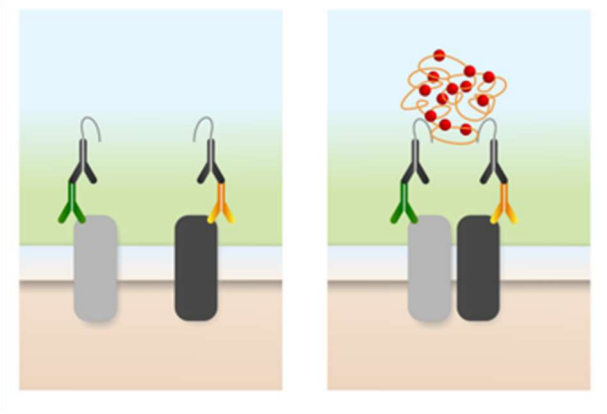

Supplementary Fig. 3: Schematic representation of the proximity ligation assay.

The proximity ligation assay consists of incubation with primary antibody from two different species specific to the target proteins. Then, samples were incubated with secondary antibodies coupled with PLA probes and raised against the desired species. If they are in close vicinity, a connector oligonucleotide joins the PLA probes. This results in a closed circular DNA template, which is amplified using a DNA polymerase. Finally, a detection oligonucleotide coupled to a fluorochrome hybridizes to repeating sequences in the amplicon. The PLA signal was detected using fluorescence microscopy as discrete dots, which illustrates the interaction between the proteins of interest.

References

1 Thomas, C. & Tampe, R. Structural and Mechanistic Principles of ABC Transporters. *Annu Rev Biochem* **89**, 605-636, doi:10.1146/annurev-biochem-011520-105201 (2020).

2 Molday, R. S., Garces, F. A., Scortecci, J. F. & Molday, L. L. Structure and function of ABCA4 and its role in the visual cycle and Stargardt macular degeneration. *Prog Retin Eye Res*, 101036, doi:10.1016/j.preteyeres.2021.101036 (2021).

3 Kawaguchi, K. & Morita, M. ABC Transporter Subfamily D: Distinct Differences in Behavior between ABCD1-3 and ABCD4 in Subcellular Localization, Function, and Human Disease. *Biomed Res Int* **2016**, 6786245, doi:10.1155/2016/6786245 (2016).

4 Gerovac, M. & Tampe, R. Control of mRNA Translation by Versatile ATP-Driven Machines. *Trends Biochem Sci* **44**, 167-180, doi:10.1016/j.tibs.2018.11.003 (2019).

5 Csanady, L., Vergani, P. & Gadsby, D. C. Structure, Gating, and Regulation of the Cftr Anion Channel. *Physiol Rev* **99**, 707-738, doi:10.1152/physrev.00007.2018 (2019).

6 Tinker, A., Aziz, Q., Li, Y. & Specterman, M. ATP-Sensitive Potassium Channels and Their Physiological and Pathophysiological Roles. *Compr Physiol* **8**, 1463-1511, doi:10.1002/cphy.c170048 (2018).

7 Frank, N. Y. *et al.* Regulation of progenitor cell fusion by ABCB5 p-glycoprotein, a novel ATP-binding cassette transporter. *J Biol Chem* **278**, 47156-47165 (2003).

8 Schatton, T. *et al.* Identification of cells initiating human melanomas. *Nature* **451**, 345-349, doi:10.1038/nature06489 (2008).

9 Ksander, B. R. *et al.* ABCB5 is a limbal stem cell gene required for corneal development and repair. *Nature* **511**, 353-357, doi:10.1038/nature13426 (2014).

10 Frank, N. Y. *et al.* ABCB5-mediated doxorubicin transport and chemoresistance in human malignant melanoma. *Cancer Res* **65**, 4320-4333, doi:10.1158/0008-5472.CAN-04-3327 (2005).

11 Yang, J. Y., Ha, S. A., Yang, Y. S. & Kim, J. W. p-Glycoprotein ABCB5 and YB-1 expression plays a role in increased heterogeneity of breast cancer cells: correlations with cell fusion and doxorubicin resistance. *BMC Cancer* **10**, 388, doi:10.1186/1471-2407-10-388 (2010).

12 Wilson, B. J. *et al.* ABCB5 identifies a therapy-refractory tumor cell population in colorectal cancer patients. *Cancer Res* **71**, 5307-5316, doi:10.1158/0008-5472.CAN-11-0221 (2011).

13 Kugimiya, N. *et al.* The c-MYC-ABCB5 axis plays a pivotal role in 5-fluorouracil resistance in human colon cancer cells. *J Cell Mol Med* **19**, 1569-1581, doi:10.1111/jcmm.12531 (2015).

14 Cheung, S. T., Cheung, P. F., Cheng, C. K., Wong, N. C. & Fan, S. T. Granulin-epithelin precursor and ATP-dependent binding cassette (ABC)B5 regulate liver cancer cell chemoresistance. *Gastroenterology* **140**, 344-355, doi:10.1053/j.gastro.2010.07.049 (2011).

15 Farawela, H. M., Khorshied, M. M., Kassem, N. M., Kassem, H. A. & Zawam, H. M. The clinical relevance and prognostic significance of adenosine triphosphate ATP-binding cassette (ABCB5) and multidrug resistance (MDR1) genes expression in acute leukemia: an Egyptian study. *J Cancer Res Clin Oncol* **140**, 1323-1330, doi:10.1007/s00432-014-1694-3 (2014).

16 Yang, M. *et al.* Expression of ABCB5 gene in hematological malignances and its significance. *Leuk Lymphoma* **53**, 1211-1215, doi:10.3109/10428194.2011.637214 (2012).

17 Thierry-Mieg, D. & Thierry-Mieg, J. AceView: a comprehensive cDNA-supported gene and transcripts annotation. *Genome Biol* **7 Suppl 1**, S12 11-14, doi:10.1186/gb-2006-7-s1-s12 (2006).

18 Frank, N. Y. *et al.* Regulation of progenitor cell fusion by ABCB5 P-glycoprotein, a novel human ATP-binding cassette transporter. *J Biol Chem* **278**, 47156-47165, doi:10.1074/jbc.M308700200 (2003).

19 Chen, K. G. *et al.* Principal expression of two mRNA isoforms (ABCB 5alpha and ABCB 5beta) of the ATP-binding cassette transporter gene ABCB 5 in melanoma cells and melanocytes. *Pigment Cell Res* **18**, 102-112, doi:10.1111/j.1600-0749.2005.00214.x (2005).

20 Kawanobe, T. *et al.* Expression of human ABCB5 confers resistance to taxanes and anthracyclines. *Biochem Biophys Res Commun* **418**, 736-741, doi:10.1016/j.bbrc.2012.01.090 (2012).

21 Moitra, K. *et al.* Differential gene and microRNA expression between etoposide resistant and etoposide sensitive MCF7 breast cancer cell lines. *PLoS One* **7**, e45268, doi:10.1371/journal.pone.0045268 (2012).

22 Gillet, J. P., Efferth, T. & Remacle, J. Chemotherapy-induced resistance by ATP-binding cassette transporter genes. *Biochim Biophys Acta* **1775**, 237-262, doi:10.1016/j.bbcan.2007.05.002 (2007).

23 Keniya, M. V. *et al.* Drug resistance is conferred on the model yeast Saccharomyces cerevisiae by expression of full-length melanoma-associated human ATP-binding cassette transporter ABCB5. *Mol Pharm* **11**, 3452-3462, doi:10.1021/mp500230b (2014).

24 Urlinger, S., Kuchler, K., Meyer, T. H., Uebel, S. & Tampé, R. Intracellular location, complex formation, and function of the transporter associated with antigen processing in yeast. *Eur j Biochem* **245**, 266-272 (1997).

25 Maio, N., Kim, K. S., Holmes-Hampton, G., Singh, A. & Rouault, T. A. Dimeric ferrochelastase bridges ABCB7 and ABCB10 homodimers in an architecturally defined molecular complex required for hemme biosynthesis. *Haematologica* **104**, 1756-1767 (2019).

26 Elliott, A. M. & Al-Hajj, M. A. ABCB8 mediates doxorubicin resistance in melanoma cells by protecting the mitochondrial genome. *Mol Cancer Res* **7**, 79-87 (2009).

27 Minami, K. *et al.* Expression of ABCB6 is related to resistance to 5-FU, SN-38 and vincristine *Anticancer Res* **34**, 4767-4773 (2014).

28 Gong, J.-P. *et al.* Overexpression of microRNA-24 increases the sensitivity to paclitaxel in drug-resistant breast carcinoma cell lines via targeting ABCB9. *Oncol Lett* **12**, 3905-3911 (2016).

29 Bergam, P. *et al.* ABCB6 resides in melanosomes and regulates early steps of melanogenesis required for PMEL amyloid matrix formation. *J Mol Biol* **430**, 3802-3818 (2018).

30 Zhang, C. *et al.* Mutations in ABCB6 cause dyschromatosis universalis hereditaria. *J Invest Dermatol* **133**, 2221-2228 (2013).

31 Chen, K. G., Valencia, J. C., Gillet, J.-P., Hearing, V. J. & Gottesman, M. M. Involvement of ABC transporters in melanogenesis and the development of multidrug resistance of melanoma *Pigment Cell Melanoma Res* **22**, 740-749 (2010).

32 Chen, K. G. *et al.* Melanosomal sequestration of cytotoxic drugs contributes to the intractability of malignant melanomas. *PNAS* **103**, 9903-9907 (2006).

33 King, C., Raicu, V. & Hristova, K. Understanding the FRET signatures of interacting membrane proteins. *J Biol Chem* **292**, 5291-5310 (2017).

34 Machleidt, T. *et al.* NanoBRET - A novel platform for the analysis of protein-protein interactions *ACS Chem Biol* **10**, 1797-1804 (2015).

35 Hillebrand, M. *et al.* Live cell FRET microscopy: homo- and heterodimerization of two human peroxisomal ABC transporters, the adrenoleukodystrophy protein (ALDP, ABCD1) and PMP70 (ABCD3). *J Biol Chem* **282**, 26997-27005, doi:10.1074/jbc.M702122200 (2007).

36 Krishnamurthy, P. C. *et al.* Identification of a mammalian mitochondrial porphyrin transporter. *Nature* **443**, 586-589 (2006).

37 Paterson, J. K. *et al.* Human ABCB6 localizes to both the outer mitochondrial membrane and the plasma membrane. *Biochemistry* **46**, 9443-9452, doi:10.1021/bi700015m (2007).

38 Kiss, K. *et al.* Shifting the paradigm: the putative mitochondrial protein ABCB6 resides in the lysosomes of cells and in the plasma membrane of erythrocytes. *PLoS One* **7**, e37378, doi:10.1371/journal.pone.0037378 (2012).

39 Graab, P. *et al.* Lysosomal targeting of the ABC transporter TAPL is determined by membrane-localized charged residues. *J Biol Chem* **294**, 7308-7323 (2019).

40 Gomes, I., Sierra, S. & Devi, L. A. Detection of receptor heterodimerization using in situ proximity ligation assay. *Curr Protoc Pharmacol* **75** (2016).